

Structural and magnetic properties of La_{0.7}Sr_{0.3}MnO₃ thin films integrated onto Si(100) substrates with SrTiO₃ as buffer layer

M. Belmeguenai, S. Mercone, C. Adamo, P. Moch, D. G. Schlom, and P. Monod

Citation: *Journal of Applied Physics* **109**, 07C120 (2011); doi: 10.1063/1.3565422

View online: <http://dx.doi.org/10.1063/1.3565422>

View Table of Contents: <http://scitation.aip.org/content/aip/journal/jap/109/7?ver=pdfcov>

Published by the **AIP Publishing**

Articles you may be interested in

Enhanced electrical and magnetic properties in La_{0.7}Sr_{0.3}MnO₃ thin films deposited on CaTiO₃-buffered silicon substrates

APL Mat. **3**, 062504 (2015); 10.1063/1.4915486

Controlling magnetic anisotropy in La_{0.7}Sr_{0.3}MnO₃ nanostructures

Appl. Phys. Lett. **104**, 052408 (2014); 10.1063/1.4863978

Control of the magnetization in pre-patterned half-metallic La_{0.7}Sr_{0.3}MnO₃ nanostructures

J. Appl. Phys. **112**, 103921 (2012); 10.1063/1.4765672

Nanoscale magnetic structure and properties of solution-derived self-assembled La_{0.7}Sr_{0.3}MnO₃ islands

J. Appl. Phys. **111**, 024307 (2012); 10.1063/1.3677985

Microstructural and magnetic properties of (La_{0.7}Sr_{0.3}MnO₃)_{0.7}:(Mn₃O₄)_{0.3} nanocomposite thin films

J. Appl. Phys. **109**, 054302 (2011); 10.1063/1.3552594

You don't still use this cell phone

or this computer

Why are you still using an AFM designed in the 80's?

It is time to upgrade your AFM

Minimum \$20,000 trade-in discount for purchases before August 31st

Asylum Research is today's technology leader in AFM

dropmyoldAFM@oxinst.com

OXFORD INSTRUMENTS
The Business of Science®



Structural and magnetic properties of $\text{La}_{0.7}\text{Sr}_{0.3}\text{MnO}_3$ thin films integrated onto Si(100) substrates with SrTiO_3 as buffer layer

M. Belmeguenai,^{1,a)} S. Mercone,¹ C. Adamo,² P. Moch,¹ D. G. Schlom,² and P. Monod³

¹LSPM, UPR 3407 CNRS, Université Paris 13, Av. J.-B. Clément, 93430 Villetaneuse, France

²Department of Materials Science and Engineering, Cornell University, Ithaca, New York 14853-1501, USA

³LPEM, UPR A0005 CNRS, ESPCI, 10 Rue Vauquelin, F-75231 Paris cedex 5, France

(Presented 18 November 2010; received 23 September 2010; accepted 3 January 2011; published online 11 April 2011)

$\text{La}_{0.7}\text{Sr}_{0.3}\text{MnO}_3$ (LSMO) thin films with a thickness d of 10, 20, 60, and 100 nm were grown on 20-nm-thick SrTiO_3 -buffered (100) silicon substrates by a reactive molecular beam epitaxy. For all samples, x-ray diffraction (XRD) revealed an excellent epitaxy with in-plane cubic [100] and [010] axes of LSMO. The XRD measured values of the out-of-plane lattice parameter suggest that the strain state does not vary significantly from sample to sample. A superconducting quantum interference device reveals that the room temperature magnetization at saturation increases with d and nearly reaches the bulk value for $d = 100$ nm; the Curie temperature ranges in the 320–350 K interval, to compare to 360 K in the bulk. Ferromagnetic resonance (FMR) in cavity (at 9.5 GHz) and microstrip FMR used to investigate the dynamic magnetic properties, revealed a fourfold anisotropy showing its easy axes along the [110] and $[1\bar{1}0]$ directions. In the thickest samples ($d > 20$ nm), the FMR spectra present two distinct resonant modes. This splitting is presumably due to the simultaneous presence of two different magnetic phases. © 2011 American Institute of Physics. [doi:10.1063/1.3565422]

$\text{La}_{0.7}\text{Sr}_{0.3}\text{MnO}_3$ (LSMO), which belongs to the family of the perovskitelike manganites, is expected to present a spin polarization close to 100% (half metal).¹ This material has been therefore used in a number of spin-dependent transport devices grown on insulating and matching substrates [SrTiO_3 (STO) and NdGaO_3] such as magnetic tunneling junctions^{1,2} and spin valves.^{3,4} Moreover, LSMO is a good candidate for spin injection into semiconductors, due to its low carrier density, its high spin polarization of charge carriers, and its ferromagnetism at the room temperature.⁵ Therefore, the integration of LSMO as a source of spin polarized carriers in semiconductor based devices is a challenging task for potential applications utilizing both information processing and data storage in the same device, such as high-density magnetic memories and magnetic sensors.

In order to grow an epitaxial quality manganite film on a semiconductor substrate, the film–substrate lattice mismatch needs to be minimized and chemical reactions between the substrate and the deposited film should be eliminated. The first attempts in order to obtain the epitaxial LSMO films on Si used a buffer intermediate layer consisting of STO or of Yttria stabilized zirconia (YSZ)^{6,7} while other ones⁸ took advantage of the SiO_x native oxide film on the Si surface. Due the recent progresses concerning the direct integration^{9,10} of STO on Si, the STO buffer layers are now often for integrating LSMO onto this technologically important semiconductor. Up to now, the intense research activity on LSMO thin films grown on Si substrates^{11–13} was mainly focused on their structural and static magnetic properties, but according to our knowledge their dynamic magnetic proper-

ties remain unexplored. Therefore, the aim of this paper is to investigate static and dynamic magnetic properties of LSMO thin films of various thicknesses deposited on a Si substrate preliminary overlaid with a thin STO buffer.

LSMO films (with a thickness d of 10, 20, 60, and 100 nm) were grown on Si (001) substrates by a reactive molecular beam epitaxy (MBE) system using 20-nm-thick STO template layers. The x-ray diffraction (XRD) study shows that all the LSMO films are fully (001) oriented and of high epitaxial quality. The identical value of the out-of-plane lattice parameter, measured using XRD in the geometry θ – 2θ , reveals that all the films are subjected to nearly equal in-plane tensile epitaxial strains. The pole figures measured around the {110} peak show a full in-plane epitaxy with LSMO [100] and [010] cubic axes along the sample edges. Therefore, from this x-ray study, a fourfold in-plane magnetic anisotropy, for which one principal axis which can be chosen parallel to the [110] direction, is expected.

The static magnetic properties were measured up to 400 K, using a superconducting quantum interference device (SQUID). The dynamic measurements were carried out through conventional ferromagnetic resonance (FMR) and microstrip line FMR (MS-FMR) techniques.¹⁴ The FMR setup consists of a bipolar X-band Bruker ESR spectrometer with a TE_{102} resonant cavity immersed in an Oxford cryostat allowing for exploring the 4–300 K temperature interval. The MS-FMR setup consists of a home-made mounting which, up to now, only works at the room temperature.

The measured Curie temperatures (T_c) range in the 320–350 K interval (Fig. 1). The room-temperature magnetization at saturation increases with the thickness and nearly reaches the bulk value for $d = 100$ nm (see Table I).

^{a)}Author to whom correspondence should be addressed. Electronic mail: belmeguenai.mohamed@univ-paris13.fr.

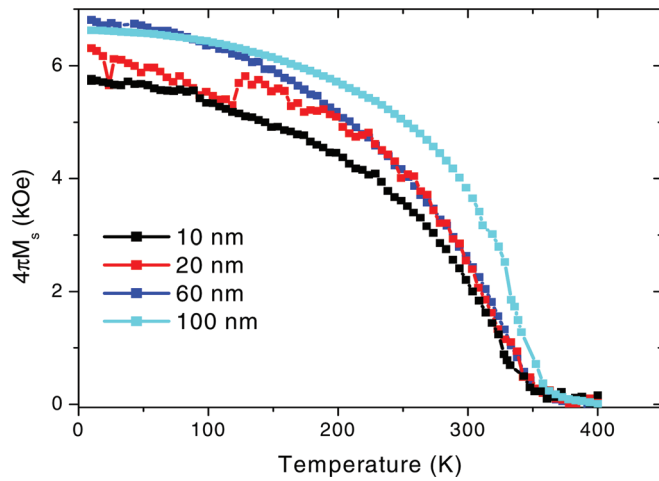


FIG. 1. (Color online) Temperature dependences of $4\pi M_s$ in LSMO films measured under a 5000 Oe in-plane applied field.

As previously published,¹⁵ the dynamic properties are tentatively interpreted assuming a magnetic energy density which, in addition to Zeeman and demagnetizing contributions, contains a perpendicular and an in-plane anisotropy contribution

$$E = -M_s H [\sin \theta_M \sin \theta_H \cos(\varphi_M - \varphi_H) + \cos \theta_M \cos \theta_H] - (2\pi M_s^2 - K_\perp) \sin^2 \theta_M - \frac{1}{8} K_4 (3 + \cos 4(\varphi_M - \varphi_4)) \sin^4 \theta_M \quad (1)$$

As detailed in Ref. 15, θ_M and ϕ_M , respectively, represent the out-of-plane angle and the in-plane angle (referring to the [100] axis) defining the direction of the magnetization M_s ; ϕ_4 stands for the angle between a fourfold easy axis with the [100] direction. K_4 is chosen positive with this definition. As in Ref. 15 we introduce the effective magnetization field $4\pi M_{\text{eff}} = 4\pi M_s - 2K_\perp/M_s = 4\pi M_s - H_\perp$ and the fourfold in-plane anisotropy field $H_4 = 4K_4/M_s$.

The H in-plane and H out-of-plane MS-FMR spectra of all the samples reveal a single uniform precession mode, except for the 100-nm-thick film for which an additional mode is observed. In this last sample, the lower and the higher frequency modes are called mode 1 and mode 2, respectively: With an in-plane applied field, their frequency difference increases with H in such a way that, due to their experimentally observed line-widths, the two modes cannot be clearly resolved for $H < 400$ Oe (Fig. 2(a)). For H normal to the sample plane (and large enough to allow for $M_s//H$) the measured frequencies linearly vary versus H , as expected from the studied model [Fig. 2(b)]. In the 100-nm-thick film, the frequency difference between mode 1 and mode 2 is independent of H .

Additional investigations relative to the temperature dependence of the resonance spectra were performed using conventional FMR. Depending on the temperature and on the studied film, these spectra show one or two uniform modes: In the 100-nm-thick sample, the occurrence of two modes is restricted to the 240–300 K interval, while, for the 60-nm-thick film, such a multiplicity only advects in the

TABLE I. Magnetic parameters at room temperature obtained from the best fits to our experimental results (n.m.: not measured). H_\perp is calculated using the $4\pi M_{\text{eff}}$ values derived from in-plane measurements.

| Thickness (nm) | 10 nm | 20 nm | 60 nm | 100 nm | |
|---|-------|-------|-------|--------|--------|
| | | | | Mode 1 | Mode 2 |
| $4\pi M_s$ (kOe) | 2.4 | 2.85 | 2.8 | 4 | |
| $4\pi M_{\text{eff}}$ (kOe) (MS-FMR: out-of-plane) | n.m. | 4.9 | 4.9 | 4.7 | 5.6 |
| $4\pi M_{\text{eff}}$ (kOe) (MS-FMR: in-plane) | 4.6 | 4.9 | 4.9 | 5 | 6 |
| H_\perp (kOe) | -2.2 | -2 | 2.1 | -1 | -2 |
| H_4 (Oe) | 50 | 8 | 28 | 30 | 38 |

120–200 K region and, for the other samples, is always absent. These differences are not yet fully understood. Anyway, a critical analysis of the experimental results clearly argues for the uniform character of both modes when the two above mentioned distinct resonances are observed.

The four studied samples present very similar structural and magnetic characteristics, except for the above mentioned multiplicity appearing in the thickest films (60 and 100 nm). In the following the experimental results concerning these two last samples which show an unusually richer behavior will benefit of a more detailed description. Anyway, an exhaustive list of the derived significant magnetic parameters can be found on Table I.

The MS-FMR technique, in perpendicular configuration, allows for deriving the values of the effective Landé factor g and of the effective demagnetizing field $4\pi M_{\text{eff}}$ from the variation of the resonance frequency versus the magnitude of the applied field. Such typical dependences are shown on Fig. 2(b). The Landé factor is found independent of the sample ($g = 1.915$) but $4\pi M_{\text{eff}}$ substantially varies: The deduced values of $4\pi M_{\text{eff}}$ are reported in Table I. Taking into account the static magnetization reported above it results that (H_\perp) is negative (thus implying a perpendicular easy plane uniaxial anisotropy). Its main source seems to be related to the interfacial strain through the magneto-elastic coupling. It can be easily proved that, due to the order of magnitude of the magnetic parameters and of the available applied fields, the in-plane geometry does not allow for a precise simultaneous determination of g and of $4\pi M_{\text{eff}}$. However, in this geometrical configuration, if g is fixed (1.915 in the present case), for large values of H a good agreement between measured and expected frequency variations versus the applied field can be obtained using appropriately chosen effective demagnetizing fields. These fields are also reported in Table I: In some cases they slightly differ (up to 400 Oe) from the derived ones using the previously mentioned perpendicular geometry. These differences are presumably related to the small unavoidable misalignment between the applied field and the direction normal to the sample plane which induces errors in the determination of g and of $4\pi M_{\text{eff}}$ in perpendicular geometry. According to our simulations, an error of 5% results from a misalignment of 1° .

MS-FMR can be performed over a large frequency range, thus allowing for eventually applying small in-plane

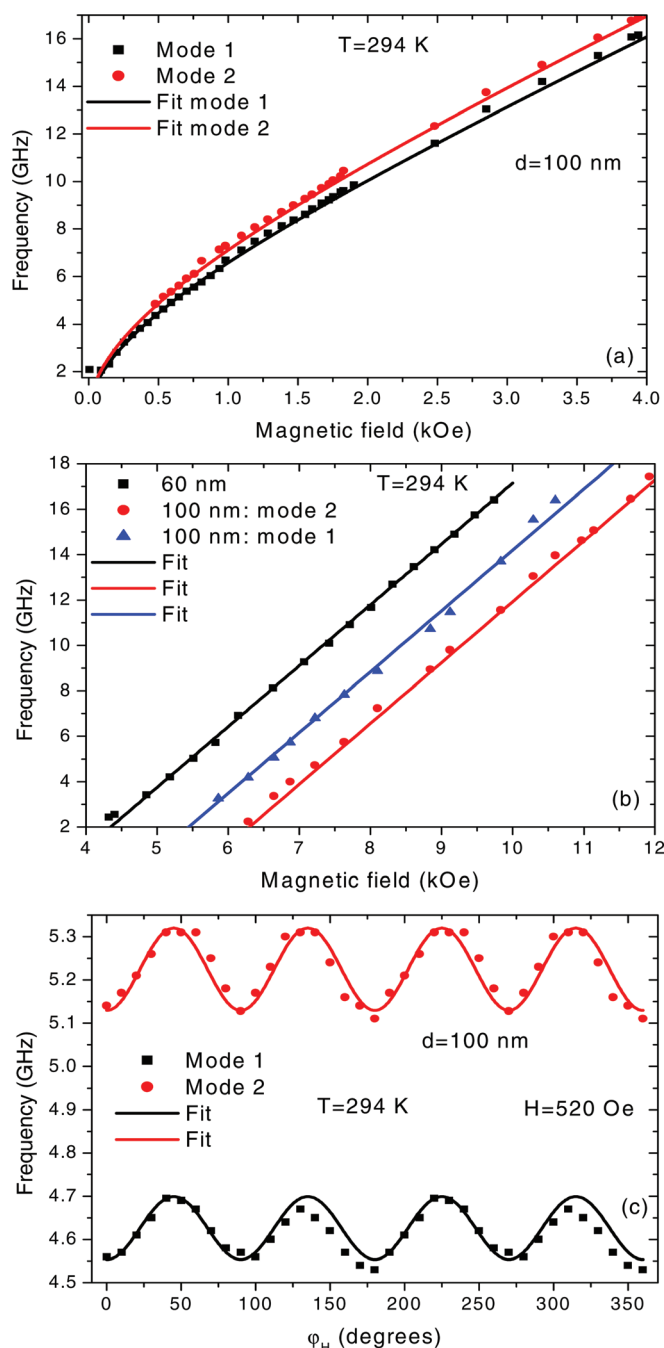


FIG. 2. (Color online) Field dependence of the resonance frequency of the uniform excited modes of the 60-nm and 100-nm-thick LSMO films. The magnetic field is applied (a) in-plane and (b) perpendicular to the film plane. (c) In-plane angular dependence of the resonance frequency of the uniform modes of the 100-nm-thick LSMO film. Fits are obtained using the parameters indicated in the Table I.

magnetic fields in order to put in evidence rather weak magnetic anisotropies which cannot be detected using the high applied magnetic fields required in conventional FMR. Taking an advantage of this opportunity, we derived the in-plane anisotropy at the room temperature of all the samples from the resonance frequency variations versus the direction (defined by φ_H) of an in-plane applied field of a small fixed amplitude. Figure 2(c) shows such typical experimental angular dependences in the 100-nm-thick sample. For all the

investigated films the experimental data are satisfactorily fitted using the model described in Ref. 15 on the basis of Eq. (1). In all the cases we find: $\varphi_4 = 45^\circ$, which means that the [110] (and, indeed, the $[1\bar{1}0]$) direction defines a principal axis, as expected from our XRD study and, moreover, that it corresponds to an easy direction. The values derived for H_4 are reported in Table I. Notice that in the 100-nm, H_4 gets different values in mode 1 and mode 2. This is confirmed by additional measurements at lower temperature using conventional FMR. This result confirms the hypothesis that both modes are uniform modes with distinct effective demagnetizing fields and distinct anisotropies and excludes, for instance, the identification of mode 2 to a perpendicular standing excitation. Consequently, we think that, at least in some temperature and thickness ranges, two different magnetic phases can coexist and that they define distinct uniform modes showing different effective demagnetizing and anisotropy fields.

The occurrence of two modes in the thickest samples prevents for deriving unambiguous conclusions concerning the influence of the thickness d on the magnetic parameters. However, as illustrated on Table I, the magnetization M_s tends to decrease when d decreases, as generally observed, and the anisotropy fields tend to increase, which argue for their interfacial character inducing a partial relaxation along a direction normal to the film and, consequently, their enhanced effective values when d is reduced. A quantitative model, taking in account the energy terms related to the interfacial strains evoked in Ref. 15, is presumably too ambitious, regarding to the observed dispersion of the experimental results.

The temperature dependence of the static and dynamic magnetic properties of 10, 20, 60 and 100-nm-thick LSMO films, deposited on Si substrates overlaid by a 20 nm STO buffer layer have been studied. Our x-ray diffraction measurements show an excellent epitaxial (001) orientation of the LSMO films. The magnetic behavior is interpreted assuming a magnetic energy density characterized by a strong uniaxial anisotropy along the direction normal to the plane of the films and by an in-plane anisotropy showing a fourfold symmetry. The four studied samples present very similar structural and magnetic characteristics, except for the unusual presence of two uniform magnetic resonance modes in the thickest samples. This mode multiplicity arises from the presence of two distinct magnetic phases.

- ¹M. Bowen *et al.*, *Appl. Phys. Lett.* **82**, 233 (2003).
- ²Y. Ishii *et al.*, *Appl. Phys. Lett.* **87**, 22509 (2005).
- ³Z. H. Xiong *et al.*, *Nature* **427**, 821 (2004).
- ⁴V. Dediu *et al.*, *Solid State Commun.* **122**, 181 (2002).
- ⁵J.-H. Park *et al.*, *Phys. Rev. Lett.* **81**, 1953 (1998).
- ⁶J. Fontcuberta *et al.*, *J. Appl. Phys.* **85**, 4800 (1999).
- ⁷Z. Trajanovic *et al.*, *Appl. Phys. Lett.* **69**, 1005 (1996).
- ⁸I. Bergenti *et al.*, *Curr. Appl. Phys.* **7**, 47 (2007).
- ⁹J.-H. Kim *et al.*, *Appl. Phys. Lett.* **82**, 4295 (2003).
- ¹⁰Y. Wang *et al.*, *Appl. Phys. Lett.* **80**, 97 (2002).
- ¹¹A. K. Pradhan *et al.*, *J. Appl. Phys.* **103**, 023914 (2008).
- ¹²I. Bergenti *et al.*, *Prog. Solid State Chem.* **33**, 293 (2005).
- ¹³I. Bergenti *et al.*, *Curr. Appl. Phys.* **7**, 47 (2007).
- ¹⁴M. Belmeguenai *et al.*, *Phys. Rev. B* **79**, 024419 (2009).
- ¹⁵M. Belmeguenai *et al.*, *Phys. Rev. B* **81**, 054410 (2010).